



Platinum Integrated Graphene for Methanol Fuel Cells

Shang, N., Papakonstantinou, P., Wang, P., & Silva, SRP. (2010). Platinum Integrated Graphene for Methanol Fuel Cells. *Journal Of Physical Chemistry C*, 114(35), 15837-15841. <https://doi.org/10.1021/jp105470s>

[Link to publication record in Ulster University Research Portal](#)

Published in:
Journal Of Physical Chemistry C

Publication Status:
Published (in print/issue): 01/08/2010

DOI:
[10.1021/jp105470s](https://doi.org/10.1021/jp105470s)

Document Version
Publisher's PDF, also known as Version of record

General rights
Copyright for the publications made accessible via Ulster University's Research Portal is retained by the author(s) and / or other copyright owners and it is a condition of accessing these publications that users recognise and abide by the legal requirements associated with these rights.

Take down policy
The Research Portal is Ulster University's institutional repository that provides access to Ulster's research outputs. Every effort has been made to ensure that content in the Research Portal does not infringe any person's rights, or applicable UK laws. If you discover content in the Research Portal that you believe breaches copyright or violates any law, please contact pure-support@ulster.ac.uk.

Platinum Integrated Graphene for Methanol Fuel Cells

Naigui Shang*

Advanced Technology Institute (ATI), University of Surrey, Guildford, Surrey, GU2 7XH, U.K., and Nanotechnology and Integrated Bio-Engineering Centre (NIBEC), University of Ulster, Newtownabbey BT37 0QB, U.K.

Pagona Papakonstantinou

NIBEC, University of Ulster, Shore Road, Newtownabbey BT37 0QB, U.K.

Peng Wang

UK SuperSTEM, Daresbury Laboratory, Cheshire WA4 4AD, U.K.

S. Ravi. P. Silva

ATI, University of Surrey, Guildford, Surrey GU2 7XH, U.K.

Received: June 14, 2010; Revised Manuscript Received: August 11, 2010

Uniform and porous graphene nanoflake films (GNFs) have been investigated as a support for catalytic Pt nanoclusters in direct methanol electro-oxidation. Pt nanoclusters of varying thickness are deposited on GNFs using magnetron sputtering, and their effects on the electrocatalytic activity for oxidizing methanol are systemically studied. GNF supported Pt nanoclusters with ultralow catalyst loading exhibit high performance for methanol electrocatalytic oxidation with a large mass-specific peak current density and a ratio of forward to backward peak currents up to 1.4. These characteristics compare favorably to the majority of Pt–C based electrodes, except for those of carbon nanotubes with Pt decoration on both the inner and the outer wall surfaces. The results obtained are ascribed to a highly coupled network made of high-density 2–4 nm Pt monolayer nanoclusters on both the basal and edge planes of each nanoflakes of graphene. GNFs are a promising support material for developing next-generation advanced Pt based fuel cells and their relevant electrodes in the field of energy.

Introduction

Graphene has generated much interest and excitement in the science and technology community since its discovery, and identification of its unique physical structure has given rise to quantum phenomena being observed even at room temperature in 2004.¹ Besides the reported superior electrical conductivity and outstanding mechanical properties, as a monolayer thick material, graphene has a high surface-to-volume ratio and a theoretical mass-specific surface area up to 2630–2965 m² g^{−1}. This surface-to-mass ratio is much larger than that of other carbon materials such as carbon nanotubes (CNTs) and carbon black, etc.^{2,3} Thus, graphene has a unique advantage as a supporting platform for use of catalytic metallic materials to electro-oxidize methanol compared to other nanomaterials such as carbon black,⁴ carbon nanotube/nanofiber,⁵ CN_x nanotube,⁶ nanoporous gold leaf, etc.^{7–9} Recently, we have reported the high-rate growth of graphene nanoflake films (GNFs) directly on Si.¹⁰ GNFs are composed of a large quantity of vertically stacked few-layer graphene nanoflakes with highly crystalline quality and form a porous interlaced homogeneous network. The vertical orientation of graphene nanoflakes leads to the exposure of graphene edges on the surface. Combining this with their outstanding electronic conductivity, GNF offers an excellent electrochemical test bed to study surface interactions and

dynamics. In this work, GNFs are chosen as a novel support type for mediating the metal catalytic electro-oxidation of methanol. Different thicknesses of Pt nanoclusters are supported on the surface of graphene nanoflakes, and their properties are studied with the aim of optimizing various factors such as low precious metal loading, high current density, and fast mass and electron transport rate such that no compromise is made of the electrochemical activity and efficiency monitoring.

Experimental Section

GNFs with 1.2 μm thickness were grown on heavily doped Si wafers by microwave plasma chemical vapor deposition (CVD). The detailed growth conditions can be found in our previous paper.⁹ Pt nanoclusters with a range of thicknesses between 2.1 and 85.0 nm were deposited on the surface of GNFs by magnetron sputtering. The chamber had a base pressure of less than 4 × 10^{−6} Torr. The sputter process was carried out in Ar using a dc power at a pressure of about 5 × 10^{−3} Torr. The thickness of Pt nanoclusters was controlled by tuning the sputtering time and was calibrated using depositions onto a flat Si substrate under identical conditions. The surface morphology, microstructure, and chemical composition of Pt decorated GNFs were studied by a scanning electron microscope (SEM) and a 100 kV scanning transmission electron microscope (STEM) with a spherical aberration corrector. Electro-oxidation of methanol was studied in a three-electrode cell using an Autolab electrochemical workstation. A saturated Ag/AgCl solution, a Pt wire,

* To whom correspondence should be addressed. E-mail: ngshang@hotmail.com. Phone: +44-1483-689866. Fax: +44-1483689404.

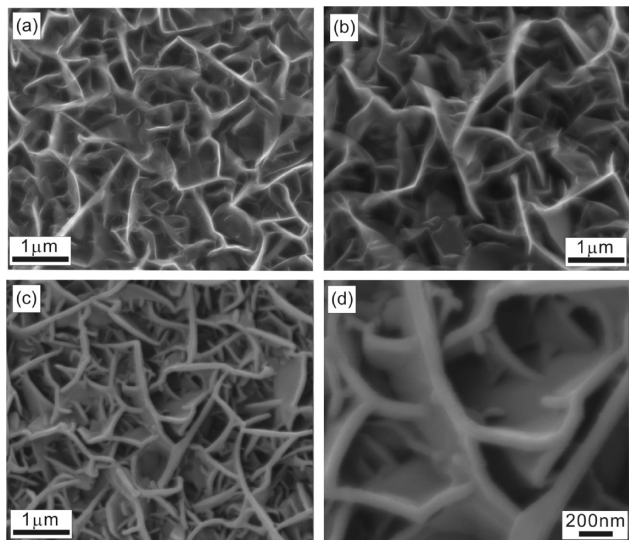


Figure 1. (a) SEM images of the pristine GNFs. (b, c) SEM images of GNFs coated by Pt nanoclusters with different thicknesses of 2.1 and 85.0 nm, respectively. (d) Enlarged SEM images of (c).

and the Pt nanocluster decorated GNF were used as the reference, counter, and working electrodes, respectively. A 10 mL cylinder cell was specially designed for use of thin film based working electrodes. The electrochemical cell with a projected working area of 0.196 cm² was sealed with a 5 mm diameter O-ring and exposed to the electrolyte. A Cu foil was tightly fixed with electrically conducting paste on the back of Si substrate entirely for good electrical contact. Before any measurements, all solutions were bubbled by flowing pure N₂ for 5–10 min and maintained under the N₂ ambient throughout the measurements. All cyclic voltammetric (CV) measurements were performed for at least five cycles, until a reliable and repeatable response was achieved. All data presented here were collected from the fifth cycle. The scan rate in all experiments is 50 mV/s.

Results and Discussion

Typical SEM images of the pristine GNFs and the Pt nanocluster decorated GNFs are shown in Figure 1. It is observed that both the pristine and Pt coated GNFs show a highly porous and wavy structure. GNFs with 2.1 nm thick Pt nanoclusters are composed of interlaced vertical, thin graphene nanoflakes, which maintain the rippled morphology of pristine GNFs. With increasing Pt nanocluster thickness, the film ripples thicken in all dimensions, manifesting a layer of uniform Pt nanoclusters coated on both the basal and edge planes of each graphene nanoflake as shown in Figure 1d. Energy dispersive X-ray spectroscopy (EDS) microprobe illustrates that the sample is composed of C and Pt elements with the characteristic energy peaks at 2.1 and 9.4 keV, respectively, as shown in the inset of Figure 2a. Elements present include O and Si, which originate from surface adsorbates and the substrate, respectively. Figure 2a,b shows low-magnification STEM images of the 2.1 nm thick Pt nanoclusters on GNFs. It is clear that the graphene nanoflakes bend, overlap, and form a petal-like scaffolding structure in a highly rippled 3D form. As-deposited Pt nanoparticles homogeneously cover the whole surface of each graphene nanoflake. The Pt nanoclusters appear to coalesce into a highly interlinked network on both the edge and basal planes of graphene nanoflakes as shown in the high-magnification STEM images of Figure 2c. The Pt nanoclusters are on average 2–4 nm in

size and are more than 4.0×10^{12} cm⁻² in areal density. The graphene nanoflakes show a distinct lattice fringe with a 0.336 nm spacing of (0002) plane, confirming they are highly graphitized and of high quality. Figure 2d shows a high angle annular dark field (HAADF) image of 2.1 nm thick Pt nanoclusters on GNFs. The Pt nanoclusters with a suitable orientation show one- or two-dimensional lattice fringes which give a 0.224 nm spacing associated with the Pt (111) plane, revealing that the Pt nanoclusters are highly crystalline and faceted. When a slightly defocused electron beam was used to observe the nanoclusters, clear lattice fringes of underlying graphenes can be observed from each of the dark void regions among the Pt nanoclusters. This is a strong evidence that the deposited Pt nanoclusters are a monolayer uniform coverage, such that this Pt–C electrode has an ultralow Pt loading less than 4.5 μg cm⁻² and a good interconnected dispersion for low-cost and highly efficient fuel cell applications.

The success of Pt nanocluster decorated graphene nanoflakes was further evidenced by a series of electrochemical CV profiles in 0.5 M H₂SO₄ shown in Figure 3a. Different from the pristine GNFs without any redox peaks, the Pt nanocluster decorated GNFs present a distinct Pt oxide reduction peak, whose potential increases from 0.404 to 0.429 V with increasing of Pt nanocluster thickness from 2.1 to 85.0 nm. This potential difference reveals the presence of a strong interaction between Pt nanoclusters and graphene nanoflakes, similar to that of other Pt–C composite electrodes. Based on this, one of the key parameters which impact on the current intensity of fuel cells, the real surface area of Pt nanoclusters that participate in the electrochemical reaction, can be determined from the charge of the Pt oxide reduction peak of 440 μC cm⁻².^{4,11,12} This method is considered to be better than that based on the hydrogen absorption/desorption peaks due to the stronger intensity and well-defined profile without a double-layer-charge induced background. Figure 3b shows the mass-specific real surface area of Pt nanoclusters as a function of the thickness from 2.1 to 85.0 nm. Note that the actual more precise mass-specific surface area could be larger than that presented here because the calculation of the Pt mass is based on a continuous and dense film without any voids. The mass-specific surface area for the 2.1 nm thick Pt nanocluster coated GNFs is largest, up to 89.9 m² g⁻¹, which is larger than that of Pt decorated CNT,^{13–15} carbon black, or graphene oxide.¹⁶ This means that the 2.1 nm thick Pt nanocluster coated GNFs have low Pt loading levels and high interconnected dispersion degree of catalysts, which are both fundamentally important for highly efficient, low-cost fuel cells. With the thickness of Pt nanoclusters from 2.1 to 85.0 nm, the mass-specific real surface substantially decreases from 89.9 to 12.6 m² g⁻¹, close to that of pure Pt materials,¹⁵ as expected based on a surface to volume argument for nanoscale device structures. The scaling is far from linear, with a 40 time reduction in nanocluster size giving rise to a surface-to-volume increase of about a factor of 7.

Figure 4a shows typical CV profiles of GNFs with different thicknesses of Pt nanoclusters for the methanol electro-oxidation in 0.5 M H₂SO₄ + 1.0 M CH₃OH using a scan rate of 50 mV/s in a potential range of 0–1.0 V. All CV profiles consist of two strong anodic peaks: a forward peak and a backward peak, which are well-known to originate from the electro-oxidation of methanol and the intermediate carbonaceous species, respectively. The 2.1 nm thick Pt decorated GNF demonstrates the highest forward and backward mass-specific peak-current densities of 11.77 and 10.76 mA cm⁻² g⁻¹, respectively. With the increase of the thickness of Pt nanoclusters, mass-specific current

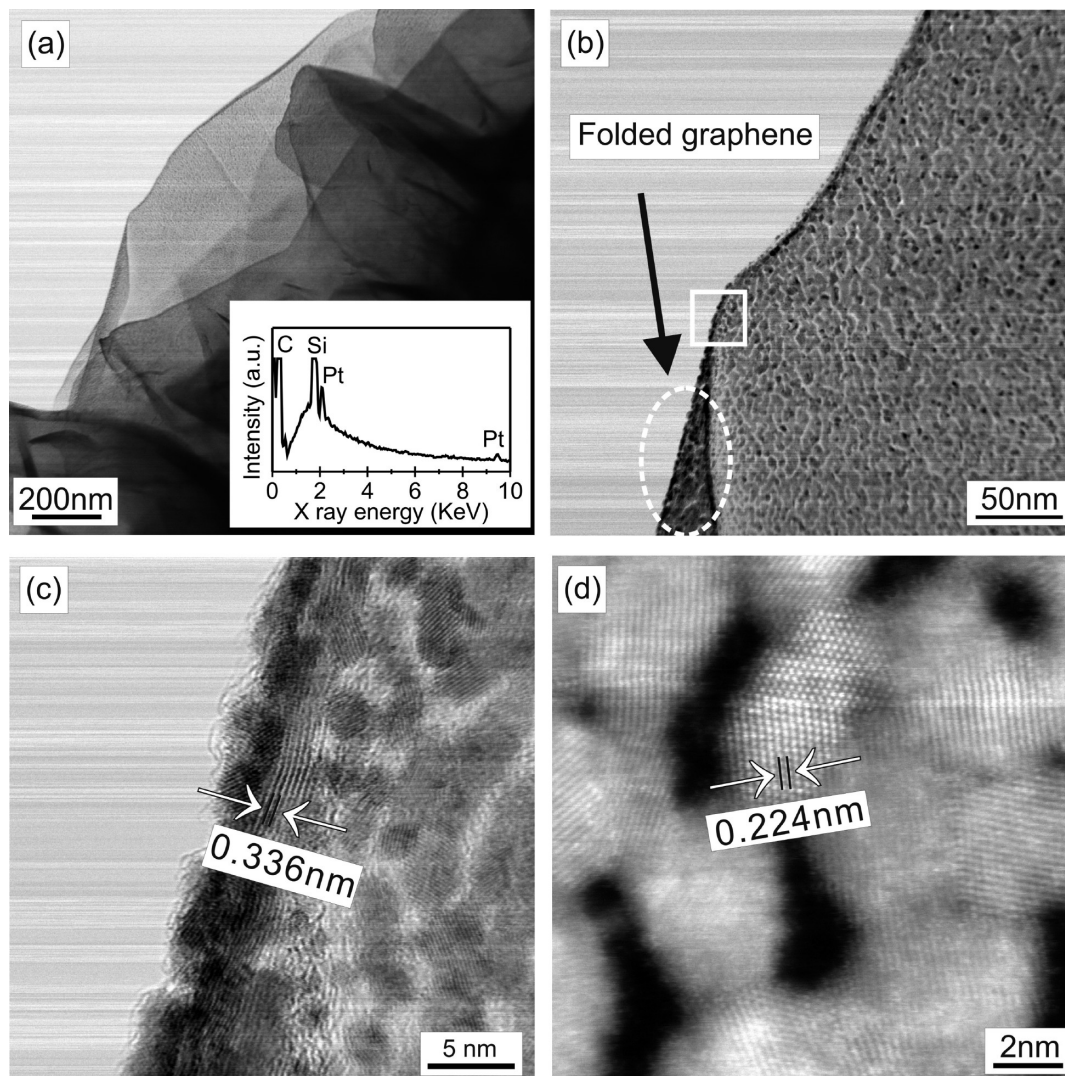


Figure 2. (a, b) Low-magnification STEM images of 2.1 nm thick Pt nanoclusters coated GNFs. Inset is the corresponding EDS spectrum taken in SEM. High-resolution STEM (c, enlarged image of the marked square area of (b)) and HAADF (d) images of 2.1 nm Pt nanoclusters on GNFs, revealing 2–4 nm monolayer Pt nanoclusters well intercoupled on both basal and edge planes of high-quality GNFs.

density of both anodic peaks greatly decreases. Figure 4b shows the mass-specific current density of methanol oxidation peak and the ratio (I_f/I_b) of forward and backward peak currents as a function of the thickness of Pt nanocluster decoration. The mass-specific peak current density significantly decreases from 11.77 to 0.48 $\text{mA cm}^{-2} \text{g}^{-1}$ at the thickness range of Pt nanoclusters of 2.1–10.6 nm and then almost keeps constant at the thickness range up to 85.0 nm. However, the ratio of forward to backward peak currents first increases from 1.09 at 2.1 nm Pt nanocluster coated GNFs to 1.39–1.41 at 5.3–10.6 nm Pt nanocluster coated GNFs and then decreases to 0.71 at the 85.0 nm Pt nanocluster coated GNFs. The I_f/I_b ratio of 1.40 ± 0.01 presented here is close to that of the Pt/C prepared by a supercritical fluid method¹⁷ and Pt nanocluster coated 10–20 layer graphene stacked nanosheets prepared by chemical reduction of exfoliated graphite oxide.⁸ The reported value here of 1.40 is larger than that of many carbon supported Pt based electrodes such as commercial Pt–C catalysts, single wall/multiwall CNT supported Pt nanoparticles,^{18–20} and costly Pt decorated nanoporous gold leaves,⁷ but less than that of template synthesized CNTs with Pt decorated inner and outer surfaces.¹⁵ The ratio is a useful fingerprint to evaluate the electrode efficiency, i.e., the tolerance of catalysts to poisoning, and has been found to basically increase with the applied anodic potential

limit.^{13,17} The larger the ratio, the more methane molecules are oxidized and the less incompletely oxidized (C–O) species accumulate on the surface of electrodes used, meaning that the electrode performs well. Another critical parameter for methanol fuel cells is the mass-specific peak current density of electrodes. The maximum mass-specific peak current density for Pt nanocluster decorated GNFs is 11.77 $\text{mA cm}^{-2} \text{g}^{-1}$, larger than that (about 1 $\text{mA cm}^{-2} \text{g}^{-1}$, calculated by the electrochemical active area and the mass activity) of Pt decorated nanoporous gold leaf.⁷ For other electrodes, this value is not available due to the unknown mass of Pt used. With the increase of thickness of Pt nanoclusters, both the I_f/I_b ratio and mass-specific current density significantly decrease. This trend is consistent with previously reported results, where support materials with large surface areas and highly dispersive coupled, small sized catalysts always possess a high activity for the electro-oxidation of methane.⁵ Increased larger size and lower dispersion of catalysts are believed to contribute to the smaller mass-specific current density and peak current ratio. Combining with the larger mass-specific current density and peak current ratio, 2.1–5.3 nm thick Pt nanocluster decorated GNFs demonstrate the best performance with a mass-specific current density of 11.77–4.12 $\text{mA cm}^{-2} \text{g}^{-1}$ and a peak current ratio of 1.09–1.39. If we make a rough calculation of the Pt loading based on a continuous dense

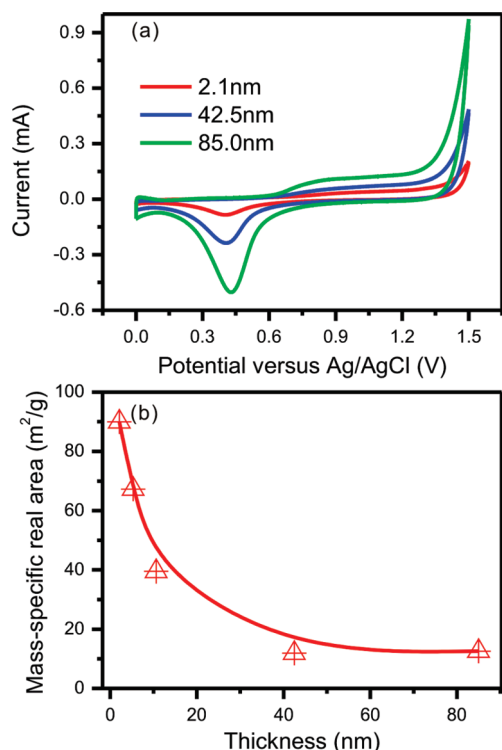


Figure 3. (a) Typical CV profiles of different thickness of Pt nanoclusters coated GNFs in 0.5 M H₂SO₄. (b) Mass-specific real area of the Pt nanoclusters coated GNFs as a function of the thickness of Pt nanoclusters.

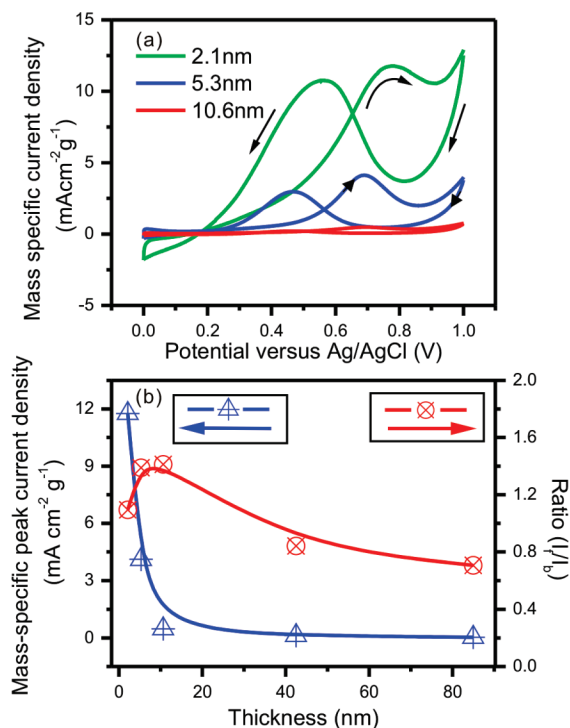


Figure 4. (a) Mass and real area double normalized CV profiles of Pt nanoclusters on GNFs for the methanol oxidation in 0.5 M H₂SO₄ + 1.0 M CH₃OH. (b) Mass-specific peak current density and ratio (I_f/I_b) of the forward and backward current intensities of Pt nanoclusters coated GNFs as a function of the thickness of Pt nanoclusters.

film on the flat substrate,²¹ the 2.1–5.3 nm thick Pt nanocluster decorated GNFs only have a catalyst loading level between 4.5 and 11.3 $\mu\text{g cm}^{-2}$, less than that of a number of highly efficient Pt–C electrodes reported previously.^{13,22} Therefore, the present

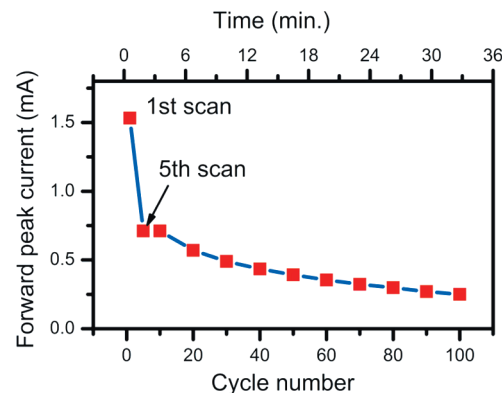


Figure 5. Forward peak current of 85 nm thick Pt nanoclusters on GNFs for the methanol oxidation in 0.5 M H₂SO₄ + 1.0 M CH₃OH as a function of both the cycle number and time.

graphene nanoflake supported Pt nanoclusters are better than the major of reported Pt–C based electrodes. In addition, the fabrication of current Pt–C electrode system is by combining the efficient GNF growth using CVD, which is followed by Pt nanocluster decoration using simple magnetron sputtering. Compared to other time-consuming, multistep methods and chemical involved, our technique is simple, highly efficient, and very facile to precisely control and to save the precious metals incorporated into devices.

The long-term stability of Pt integrated graphene electrodes has been investigated. All GNFs with different thicknesses of Pt nanoclusters have presented similar performances. Figure 5 shows the typical forward peak current of 85 nm thick Pt nanoclusters on GNFs as a function of the both cycle number and time for the methanol oxidation in 0.5 M H₂SO₄ + 1.0 M CH₃OH. It can be observed that the peak current of the methanol oxidation rapidly decreases by about 54% between the first and fifth scans and then keeps stable between the fifth and tenth scans. (For this reason, all our data used have been collected in the fifth scan.) After the tenth scan, the peak current decreases gradually with the successive scans and time. The performance is better than those of carbon nanotubes with Pt decoration on both the inner and the outer wall surfaces (about 92% loss of current after 1000 s running) and Pt/CNT composites (about 77% loss of current after 600 s running)^{15,17} and slightly poorer than that (about 72% loss of current after 1800 s running) of Pt nanocluster coated 10–20 layer graphene stacked nanosheets.⁸ The decay of peak currents with time has been ascribed to various intermediate species formed on the catalyst surface, which gradually accumulate to lower the electroactive area of catalysts, significantly poisoning the Pt nanocluster for the methanol oxidation.

The efficiency of electrodes in fuel cells is strongly related with the surface area and crystalline quality of the support materials as well as the dispersion and size of catalysts. The large surface area, high quality of supports, and highly dispersive catalysts with a nanoscale size would improve the electrode efficiency and decrease the loading level of precious metals used. In the present work, graphene nanoflakes and Pt nanoclusters help construct a new catalytic system for direct methane oxidation. Their excellent electrocatalytic activity could be ascribed to the following factors: (a) Uniform GNFs as a support possess a porous honeycomb-like surface structure and a larger surface area, preventing the Pt nanoclusters from coalescing and thus leading to form highly dispersed, high density, ultrasmall sized Pt nanoclusters with a high activity. In addition, this unique nanostructure different from CNTs and other carbon nanostruc-

tures possibly enables a certain number of oriented Pt nanoclusters deposited in order along the nanoflake surface.²³ These could provide a promotional effect to enhance the diffusion and removal of mainly carbon-, hydrogen-, and oxygen-containing catalyst poisons from the active Pt surface to graphene.²⁴ The effect could become weaker with the increase of the Pt nanocluster thickness due to the decrease of both dispersion degree and active area of Pt nanoclusters. The details are not so clear and need to be further studied by combining theoretical calculation with extensive microstructure analysis. (b) Compared to other carbon support materials, GNFs not only have a high-quality graphitized structure but also have a number of electroactive edge planes directly exposed on the surface, massively enhancing their interactions between graphene nanoflakes and Pt nanoclusters for improving the electrode efficiency.^{25,26} (c) The excellent nature of graphene,^{27,28} such as unique electronic structure, high electrical conductivity, and highly localized electronic edge state, further favors the electron transfer between the interface of graphene nanoflakes, Pt nanoclusters, and electrolytes.

Conclusion

GNFs have been used as an excellent support for Pt based fuel cells. Pt nanoclusters with different thickness have been deposited on GNFs and formed an advanced novel Pt–C hybrid electrocatalytic system by the combination of simple CVD and magnetron sputtering techniques. The hybrid films are found to exhibit distinctly superior electrocatalytic activities toward methanol oxidation with an ultralow metal loading, larger I_p/I_b ratio, and a higher mass-specific peak current compared to many Pt–C based electrodes, thus showing substantial promise as efficient electrocatalysts in direct methanol fuel cells. The improved characteristics are associated with a network of highly intercoupled Pt nanocrystals of a monolayer thickness (2–4 nm) tied with the high conductivity of graphene nanoflakes. These results should be independent of the supports used for the growth of GNFs. Si wafers as the substrate of GNFs in this work enable us to fabricate microdirect methanol fuel cell by using micro-electromechanical systems technology.²⁹ This novel graphene supported Pt based nanostructure has the potential to serve as low cost and highly efficient electrodes for direct methanol fuel cells.

Acknowledgment. Authors acknowledge support from the European Union under DESYGN-IT project (STREP Project 505626-1), EPSRC Portfolio Partnership Award, EPSRC funded facility access to UK SuperSTEM in the Daresbury Laboratory.

References and Notes

- (1) Novoselov, K. S.; Geim, A. K.; Morozov, S. V.; Jiang, D.; Zhang, Y.; Dubonos, S. V.; Grigorieva, I. V.; Firsov, A. A. *Science* **2004**, *306*, 666–669.
- (2) Peigney, A.; Laurent, C.; Flahaut, E.; Bacsa, R. R.; Rousset, A. *Carbon* **2001**, *39*, 507–514.
- (3) Chae, H. K.; Siberio-Perez, D. Y.; Kim, J.; Go, Y.; Eddaoudi, M.; Matzger, A. J.; O'Keeffe, M.; Yaghi, O. M. *Nature* **2004**, *427*, 523–527.
- (4) Park, I. S.; Lee, K. S.; Jung, D. S.; Park, H. Y.; Sung, Y. E. *Electrochim. Acta* **2007**, *52*, 5599–5605.
- (5) Wang, C. H.; Du, H. Y.; Tsai, Y. T.; Chen, C. P.; Huang, C. J.; Chen, L. C.; Chen, K. H.; Shih, H. C. *J. Power Sources* **2007**, *171*, 55–62.
- (6) Sun, C. L.; Chen, L. C.; Su, M. C.; Hong, L. S.; Chyan, O.; Hsu, C. Y.; Chen, K. H.; Chang, T. F.; Chang, L. *Chem. Mater.* **2005**, *17*, 3749–3753.
- (7) Ge, X. B.; Wang, R. Y.; Liu, P. P.; Ding, Y. *Chem. Mater.* **2007**, *19*, 5827–5829.
- (8) Yoo, E.; Okata, T.; Akita, T.; Kohyama, M.; Nakamura, J.; Honma, I. *Nano Lett.* **2009**, *9*, 2255–2259.
- (9) Xu, C.; Wang, X.; Zhu, J. W. *J. Phys. Chem. C* **2008**, *112*, 19841–19845.
- (10) Shang, N. G.; Papakonstantinou, P.; McMullan, M.; Chu, M.; Stamboulis, A.; Potenza, A.; Dhesi, S. S.; Marchetto, H. *Adv. Funct. Mater.* **2008**, *18*, 3506–3514.
- (11) Friedrich, K. A.; Henglein, F.; Stimming, U.; Unkauf, W. *Colloids Surf., A* **1998**, *134*, 193–206.
- (12) Heyd, D. V.; Harrington, D. A. *J. Electroanal. Chem.* **1992**, *335*, 19–31.
- (13) Wang, H. J.; Yu, H.; Peng, F.; Lv, P. *Electrochem. Commun.* **2006**, *8*, 499–504.
- (14) Li, X. G.; Hsing, I. M. *Electrochim. Acta* **2006**, *52*, 1358–1365.
- (15) Wen, Z. H.; Wang, Q.; Li, J. H. *Adv. Funct. Mater.* **2008**, *18*, 959–964.
- (16) Seger, B.; Kamat, P. V. *J. Phys. Chem. C* **2009**, *113*, 7990–7995.
- (17) Lin, Y. H.; Cui, X. L.; Yen, C.; Wai, C. M. *J. Phys. Chem. B* **2005**, *109*, 14410–14415.
- (18) Guo, D. J.; Li, H. L. *J. Electroanal. Chem.* **2004**, *573*, 197–202.
- (19) Mu, Y. Y.; Liang, H. P.; Hu, J. S.; Jiang, L.; Wan, L. J. *J. Phys. Chem. B* **2005**, *109*, 22212–22216.
- (20) Liu, Z. L.; Ling, X. Y.; Su, X. D.; Lee, J. Y. *J. Phys. Chem. B* **2004**, *108*, 8234–8240.
- (21) Gruber, D.; Ponath, N.; Muller, J.; Lindstaedt, F. *J. Power Sources* **2005**, *150*, 67–72.
- (22) King, J. S.; Wittstock, A.; Biener, J.; Kucheyev, S. O.; Wang, Y. M.; Baumann, T. F.; Giri, S. K.; Hamza, A. V.; Baeumer, M.; Bent, S. F. *Nano Lett.* **2008**, *8*, 2405–2409.
- (23) Du, B. C.; Tong, Y. Y. *J. Phys. Chem. B* **2005**, *109*, 17775–17780.
- (24) Zeng, J. H.; Yang, J.; Lee, J. Y.; Zhou, W. J. *J. Phys. Chem. B* **2006**, *110*, 24606–24611.
- (25) Okamoto, Y. *Chem. Phys. Lett.* **2005**, *407*, 354–357.
- (26) Park, C.; Baker, R. T. K. *J. Phys. Chem. B* **1998**, *102*, 5168–5177.
- (27) Geim, A. K.; Novoselov, K. S. *Nature Mater.* **2007**, *6*, 183–191.
- (28) Kobayashi, Y.; Fukui, K.; Enoki, T.; Kusakabe, K.; Kaburagi, Y. *Phys. Rev. B* **2005**, *71*, 193406–193409.
- (29) Tominaka, S.; Ohta, S.; Obata, H.; Momma, T.; Osaka, T. *J. Am. Chem. Soc.* **2008**, *130*, 10456–10457.

JP105470S